COBEM 2023 27TH INTERNATIONAL CONGRESS OF MECHANICAL ENGENEERING

ABCM Brazilian Society of Mechanical Sciences and Engineering
27th ABCM International Congress of Mechanical Engineering
December 04-08, 2023, Florianópolis-SC, Brazil

COB-2023-1097
EVALUATION OF DISSIMILAR WELDS WITH THE TEMPER-BEAD TECHNIQUE USING ELECTRODES ER 316L AND ER NICRMO-3 ON STEEL ASTM A182 F22

Larissa da Silva Cardoso
Humberto Vinicius Muñoz Aguirre
Italo Henrique Almeida Figueiredo
Carlos Alberto Mendes da Mota
Adelino Alves Maia Neto
Universidade Federal do Pará - UFPA, CEP: 66075-110, Rua Augusto Corrêa Nº 1, Belém, PA.
larissa.cardoso@itec.ufpa.br; humbertoaguirre23@yahoo.com.br; italoalmeida100@gmail.com; cmota@ufpa.br; adelinoalves@ufpa.br

Abstract. *An adequate procedure for the dissimilar welding must provide the buttering of the bevel which, through the temper-bead technique, enhances a thermal barrier capable of eliminating the problems of fraying the joint. The buttering interface in these welds is indicated as the most critical region of the joint due to the presence of high hardness phases, normally encountered in the coarse region of the heat affected zone (HAZ) and near the fusion line. The present work has objective to use the Higuchi and Higuchi Modified tests in the selection of operational parameters for welding controlled by the temper-bead technique in order to refine and to temper the coarse grains of the HAZ of the first layer. The coatings were deposited by the combination of two electrode wires, the ER NiCrMo-3 and the ER 316L, which used the GMAW (Gas Metal Arc Welding) process with pulsed current and with conventional current, respectively. As substrate the ASTM A182 F22 HSLA (High Strength Low Alloy) steel was used. The results showed the refinement and tempering of the HAZ of the first layer indicating the effectiveness of the technique used.*

Keywords: *Dissimilar welding; temper-bead technique, Higuchi test.*

1. INTRODUCTION

Due to the wide variety of components and transition elements, such as connectors, valves and flow regulators, found in oil refineries and thermoelectric power generation plants, there is commonly a need to weld dissimilar joints. The welding of dissimilar metals consists of joining a less noble material with another that has properties superior to those of the same.

Among the joints frequently reported for oil production and extraction plants, the ones established between austenitic stainless steels and low alloyed steels (austenitic/ferritic), which are constantly exposed to cyclic conditions and high temperatures, stand out. For these joints, the existing difference between the thermal expansion coefficients of the materials promotes a considerable accumulation of stresses during temperature variations, which can lead to premature failure of the joint. As an alternative to this problem, nickel-based filler metals, which have a coefficient of thermal expansion intermediate to austenitic stainless steels and low alloy steels, have been used because they result in a lower accumulation of residual stresses for the joint.

As one of the main factors responsible for the premature failure of austenitic/ferritic weldings, hydrogen-induced cracking or cold cracking stands out. When introduced into the molten metal, hydrogen diffuses into austenitic regions that have good solubility for the element. With rapid cooling of this region, the austenite transforms into martensite and may result in crack propagation due to the presence of hydrogen associated with a brittle microstructure.

Because of the martensitic microstructure, the heat affected zone (HAZ) of low-alloyed steels is indicated as a critical region for the propagation of hydrogen-induced cracks. Among the studies carried out in an attempt to minimize the embrittlement of the HAZ, a doctoral thesis that consisted in the application of the double layer technique stands out (Oliveira, 2013). According to the author, this technique has as its main objective to promote an adequate superposition of thermal cycles, so that the second layer promotes the refining and tempering of the HAZ with coarse grain size of the first, decreasing the sensitivity to cracking of the joint. Thus, for effective use of the technique, appropriate welding parameters must be selected for each layer.

In terms of the dissimilar interface, there are many scientific articles that address the study of the partially mixed zone partially mixed zone (PMZ) along the bond zone, with emphasis on Omar (1998), Dupont & Kusko (2007) and Kejelin et al (2007). According to these authors, one of the most usual problems at the austenitic/ferritic interface is associated

with the formation of a martensitic zone (M Zone) adjacent to the fusion line and located in the PMZ which, analogously to the HAZ, is also susceptible to hydrogen cracking.

For Dupont & Kusko (2007), the formation of the M Zone can be minimized by replacing stainless steel consumables with nickel alloys. Omar (1998) complements by stating that these regions can be eliminated by using the correct consumable and a proper preheating combination. Kejelin (2007) et al., in turn, concluded that the formation of these regions has a direct link with the welding current, and for low current levels the lower the overall dilution, which inhibits the movements of microsegregation in the initial solidification transients, and may even suppress the M zones.

Despite the susceptibility to hydrogen cracking of austenitic stainless steels, the substitution of nickel-based alloys for these steels, whenever possible, can be seen as an important factor in cost control, since nickel alloys are considerably more expensive. In this sense, the present work aims to evaluate the feasibility of combining nickel-based filler metals and austenitic stainless steel in dissimilar coating welding using the double layer technique.

2. METHODS AND MATERIALS

ASTM A182 F22 low alloy high strength steel (LAHSS) sheets in the dimensions 100 mm x 50 mm x 10 mm were used as base metal. Table 1 shows the chemical composition of this steel.

Table 1: Commercial chemical composition of ASTM A182 F22 steel (% by weight).

C	P	Mn	S	Si	Ni	Cr	Mo	Al
0,086	0,018	0,382	0,014	0,164	0,163	2,124	0,967	0,02

AWS ER NiCrMo-3 and ER 316L wire electrodes were used as filler metals, both with a diameter of 1.2 mm. Tables 2 and 3 show the commercial chemical composition of the respective wires.

Table 2: Commercial chemical composition of the NiCrMo-3 ER wire electrode (% by weight).

C	Si	Mn	Cr	Ni	P	Nb + Ta	Mo	Ti	Fe	S	Others
0,1 *	0,5 *	0,5 *	23	63,9	0,02	4,15	10	0,4 *	5,0	0,015	0,5*

(1) maximum values *

Table 3: Commercial chemical composition of AWS ER 316L wire electrode (% by weight).

C	Cr	Ni	Mo	Mn	P	S	Fe	Others
0,03 *	18,0	13,0	2,0	1,5	0,03 *	0,03 *	Balanced	0,50 *

(1) maximum values *

A mixture of 75% Ar +25% He for the NiCrMo-3 ER electrode and 98% Ar + 2% O2 for the 316L ER electrode was used as shielding gas.

2.1 Welding the isolated passes

The success of the temper-bead technique depends on proper selection of the welding parameters for the 1st and 2nd coating layer. For this to occur, the Higuchi and Modified Higuchi tests are usually used. The Higuchi test (Higuchi et al, 1980) consists in quantifying the size of the hard and soft zones of the HAZ. This quantification is obtained from a microhardness profile performed on the HAZ of a trans-versal sample, which is extracted from passes in single deposition. The Modified Higuchi test, in turn, takes into account the size of the coarse-grained and fine-grained zones of the HAZ. The Modified Higuchi test, in turn, takes into account the size of the coarse and fine grain zones of the HAZ. Thus, as suggested by Oliveira (2013), it can be said that while the Higuchi test considers criteria based on hardness, the Modified Higuchi test considers criteria based on microstructure. Thus, to pass the Higuchi test, the criteria in Equations 1 and 2 must be met, while to pass the Modified Higuchi test, the criteria in Equations 3 and 4 must be met. After quantifying the regions of interest, the decision diagrams were assembled based on the methodology proposed by Miranda (2009). These diagrams aim to select the welding conditions for the 1st and 2nd coating layer considering the Higuchi and Modified Higuchi criteria. Figure 1 presents a scheme, similar to the one developed by Aguiar (2001), with the regions of interest used to meet the Higuchi and Modified Higuchi criteria.

$PZM_2 - PZD_1 > 0$ (1)

Note: PZM_2 = second layer smooth zone depth
PZD_1 = depth of the hard zone of the first layer

$R_1 + P_1 - PZD_2 > 0$ (2)

Note: PZD_2 = depth of the hard zone of the second layer
R_1 = first layer reinforcement
P_1 = first layer penetration

$PZACGF_2 - PZACGG_1 > 0$ (3)

Note: $PZACGF_2$= HAZ depth with second layer fine grain
$PZACGG_1$ = depth of HAZ with coarse granulation of the first layer

$ZF_1 - PZACGG_2 > 0$ (4)

Note: $PZACGG_2$= depth of HAZ with coarse granulation of the second layer
ZF_1 = melted zone of the first layer

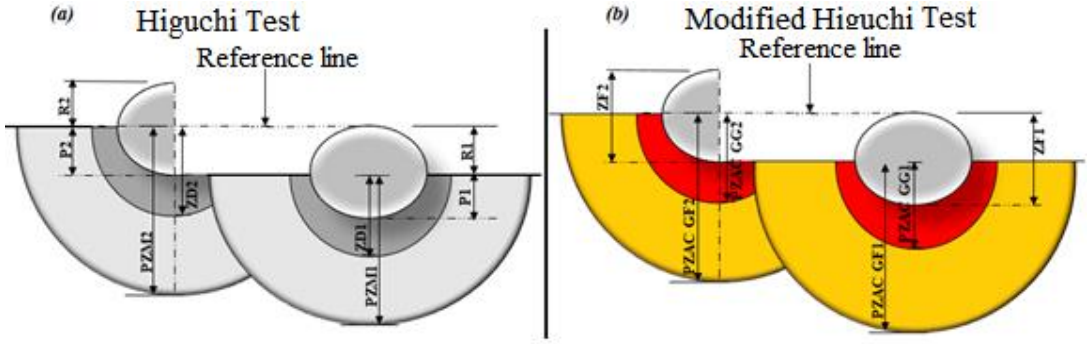

Figure 1: Illustration of the criteria of the (a) Higuchi and (b) Modified Higuchi tests.

During the deposition of isolated passes, an electronic power source and an automated displacement car were utilized. The ER 316L electrode employed the GMAW process with conventional current, whereas the ER NiCrMo-3 electrode utilized the GMAW process with pulsed current. All passes were deposited in the flat position with a pushing direction (attack angle of 75°), a contact nozzle-piece distance (CNPD) of 15 mm, and a gas flow rate of 15 l/min. Additionally, a preheating temperature of approximately 250°C was maintained. Table 4 presents the welding parameters, with the Ni nomenclature adopted for welds using the nickel electrode (ER NiCrMo-3) and the Inox nomenclature adopted for welds using the stainless steel electrode (ER 316L).

Table 4: Welding parameters adopted in the work.

Exp.	Ws(cm/min)	Fs (m/min)	Ip (A)	pt (s)	Ib (A)	bt (s)	Ia (A)	Ua (V)	Energy (J/mm)
Ni1	30	5	350	2	160	20	164	27,7	982
Ni2	30	5	350	2	135	20	151	24,8	766
Ni3	30	6	300	3	120	6	177	26,6	957
Ni4	40	6	300	3	120	6	176	26,3	710
Ni5	30	4,3	280	2,4	90	7	136	26,0	720
Ni6	40	4,3	280	2,4	90	7	134	27,7	575
Inox1	30	6	-	-	-	-	210	27	1134
Inox2	40	6	-	-	-	-	210	27	850
Inox3	50	6	-	-	-	-	210	27	680
Inox4	30	8	-	-	-	-	280	31	1736
Inox5	40	8	-	-	-	-	280	31	1336
Inox6	50	8	-	-	-	-	280	31	1041

(1) Ws represents the welding speed; Fs represents the feed speed, Ip represents the peak current; pt represents the peak time; Ib represents the base current; bt represents the base time; Ia represents the average current; Ua represents the average voltage.

The single deposition passes were sectioned into three cross-sectional samples (samples A, B, and C) that were then submitted to metallographic preparation for measurement of the geometric characteristics (strengthening, penetration, dilution), survey of the microhardness profiles along the HAZ (determination of the hard (HZ) and soft (SZ) zones), and quantification of the extent of the coarse-grained HAZ (HAZCG) and the fine-grained HAZ (HAZFG).

To quantify the extent of the hard and soft zones, microhardness tests were carried out on the cross-section sample B. As test parameters a loading of 0.1 HV, a time of 15 s, and an indentation spacing of 0.1 mm were employed. The quantification of the hard and soft zones requires the establishment of hardness values that limit the two regions. Thus, the hard zone bottom limit (HZL) and the soft zone bottom limit (SZL) were set at 310 HV and 220 HV, respectively. Finally, for the quantification of the extensions of the coarse-grained and fine-grained zones within the HAZ, the micrographs were analyzed and, with the help of the indentation line left, the extensions of the HAZCG and the HAZFG were measured.

2.2 Coating welding

It is important to note that we restricted the use of nickel electrode for the first coating layer and stainless steel electrode for the second layer. These choices are based on the results found by Dupont & Kusko (2007), which indicate the existence of larger martensitic regions at the dissimilar interface for an austenitic stainless steel alloy compared to the NiCrMo-3 ER alloy. During the making of the coatings, a 50% overlap was used between passes. Figure 2 indicates the overlap scheme adopted.

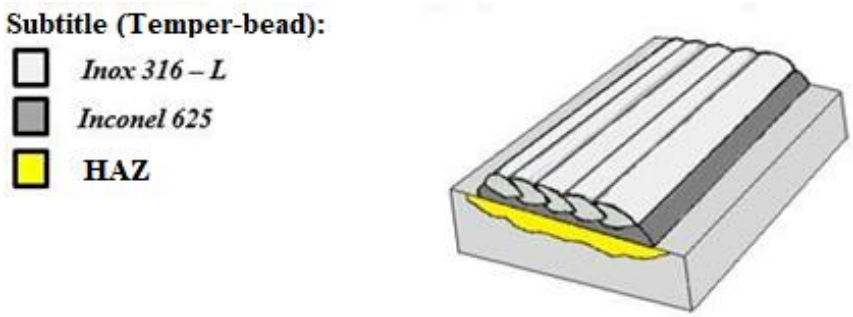

Figure 2: Schematic of the overlapping of the coating layers.

After coating welding, two cross-sectional samples were sectioned. The first served to analyze the efficiency of the temper-bead technique and the second served to evaluate a subsequent stress relief heat treatment (SRHT). Table 5 presents the conditions of the SRHT.

Table 5: SRHT parameters used in the coating sample.

Temperature (°C)	Time (min)	Type of cooling
650	120	Calm air

After the metallographic treatment, the samples were subjected to the microhardness test which consisted of a HAZ scan in the center of the third bead of the first layer with a load of 0.1 HV for 15 s and with indentation spacing of 0.1 mm.

3. RESULTS AND DISCUSSIONS

3.1 Welding the isolated passes

Figures 3 and 4 show the resulting macrographs of the cross-section B samples for the nickel and stainless steel electrodes, respectively. The macrographs show no defects of any kind. In addition, most of the strands showed good reinforcement/width ratio (R/W), with the exception of Inox 3, which had excessive convexity. The penetrations for the nickel alloy welds are lower due to the low energy levels and the current pulsation used, which tend to decrease the penetration and, consequently, the dilution. Another important factor is related to the cup-type penetration, observed in the samples deposited with the ER316L wire, which is related to the use of argon gas during welding.

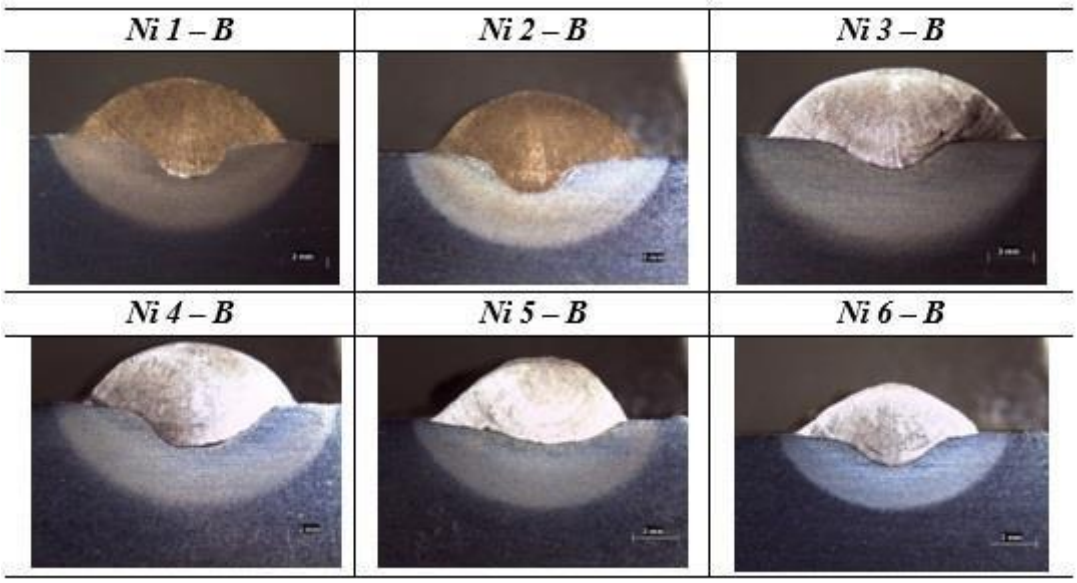

Figure 3: Macrographs of the B cross sections of the strands deposited with the NiCrMo-3 ER wire.

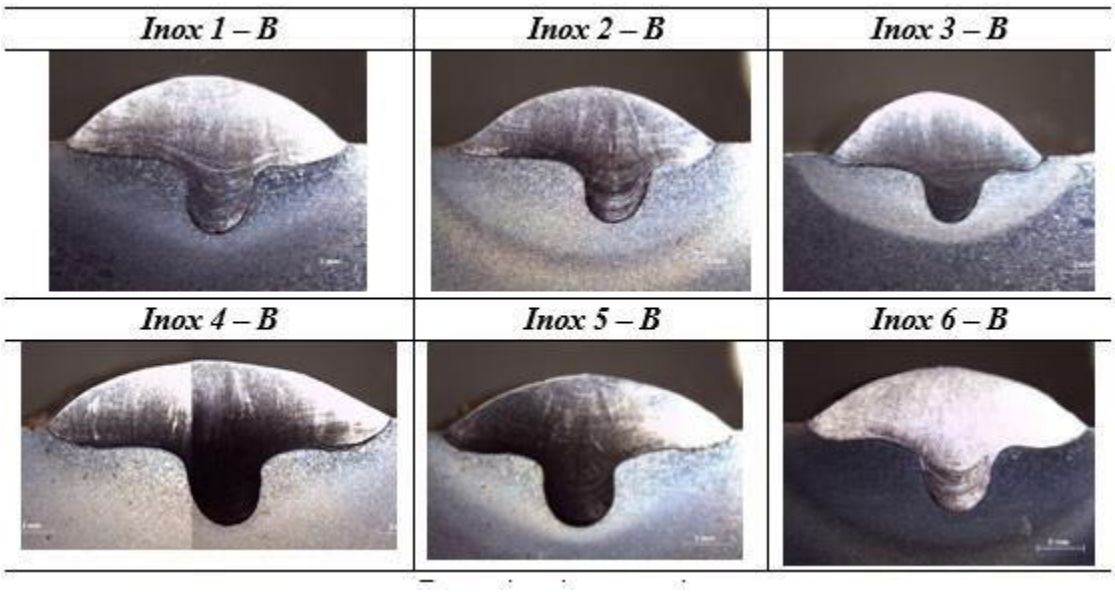

Figure 4: Macrographs of the B cross sections of the strands deposited with the ER 316L wire.

Table 6 presents the average values of width, reinforcement, and penetration determined for each welding condition. The analysis of the referred table indicates average values of reinforcement close for both electrodes, despite the significant variations in welding parameters. The penetrations, on the other hand, obtained higher values for the electrode ER 316L due, mainly, to the higher welding energies, shielding gas, and current mode selected.

Table 6: Average values of penetration, reinforcement, and width for each isolated pass.

Exp.	Width (mm)	Reinforcement (mm)	Penetration (mm)
Ni 1	10,56	2,62	2,17
Ni 2	9,61	2,78	1,47
Ni 3	11,34	3,21	1,74
Ni 4	9,48	2,69	2,10
Ni 5	8,73	2,70	1,16
Ni 6	7,82	2,1	1,50
Inox 1	12,39	2,86	3,76

Inox 2	10,65	2,54	3,33
Inox 3	8,73	2,43	2,60
Inox 4	16,86	2,62	4,55
Inox 5	13,09	2,63	4,31
Inox 6	11,94	2,63	3,84

In the region of the weld metal (WM) near the fusion line, the condition with the nickel-based electrode presents low microhardness results (less than 190 HV), but for the pass deposited with the stainless steel electrode, microhardness of an order greater than 350 HV is observed. This result suggests a more significant martensite formation for the partially mixed zone (PMZ) of the pass deposited with the stainless steel electrode, as reported by Dupont & Kusko (2007). Table 7 presents the quantified extensions of the hard zones (HZ) and soft zones (SZ) from the microhardness tests. With the results of the extensions of the DMZ and DMZ, the Higuchi diagram of Figure 5 was obtained.

Table 7: Extensions of the hard (HZ) and soft (SZ) zones in the HAZ.

Exp.	**HZ (mm)**	**SZ (mm)**
Ni 1	0,90	1,30
Ni 2	0,40	1,50
Ni 3	2,70	1,00
Ni 4	0,80	1,00
Ni 5	1,20	1,50
Ni 6	1,00	0,80
Inox 1	0,40	0,60
Inox 2	1,30	5,70
Inox 3	0,40	0,40
Inox 4	2,10	2,80
Inox 5	0,50	0,60
Inox 6	1,10	5,30

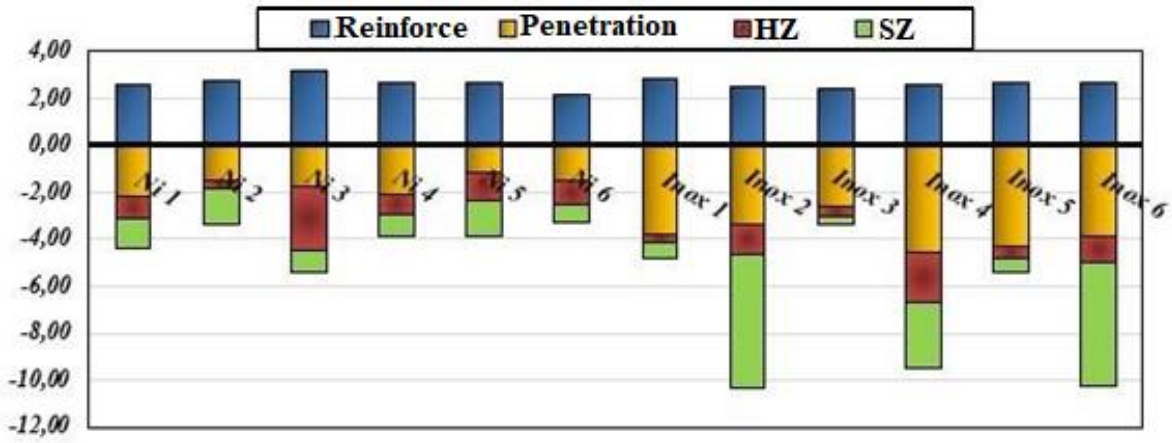

Figure 5: Higuchi diagram.

In the Higuchi diagram of Figure 5, a considerable variation in the extent of the hard and soft zones is observed, which occurs due to the different welding energy levels selected during the experimental planning. As discussed in section 2.2, it is of interest that the 316L ER wire is the second layer of coating and therefore higher energy conditions have been selected for this alloy for this alloy. Otherwise, the thermal cycling imposed by the second layer would not be able to overcome the physical barrier of the weld metal, nor would it temper the hard zone of the base metal imposed by the first coating layer.

Table 8 presents the results of the quantified extents for the coarse-grain HAZ (HAZCG) and the fine-grain HAZ (HAZFG). From the results of the extensions of the HAZCG and the HAZFG, the Modified Higuchi diagram of Figure 6 was arrived at.

Table 8: Extensions of the coarse-grained HAZ (HAZCG) and the fine-grained HAZ (HAZFG).

Exp.	GG (mm)	GF (mm)
Ni 1	0,8	1,40
Ni 2	0,70	1,20
Ni 3	2,70	1,00
Ni 4	0,90	0,90
Ni 5	1,00	1,70
Ni 6	0,90	0,90
Inox 1	0,40	0,60
Inox 2	1,20	5,80
Inox 3	0,40	0,40
Inox 4	2,20	2,70
Inox 5	0,50	0,60
Inox 6	1,20	5,20

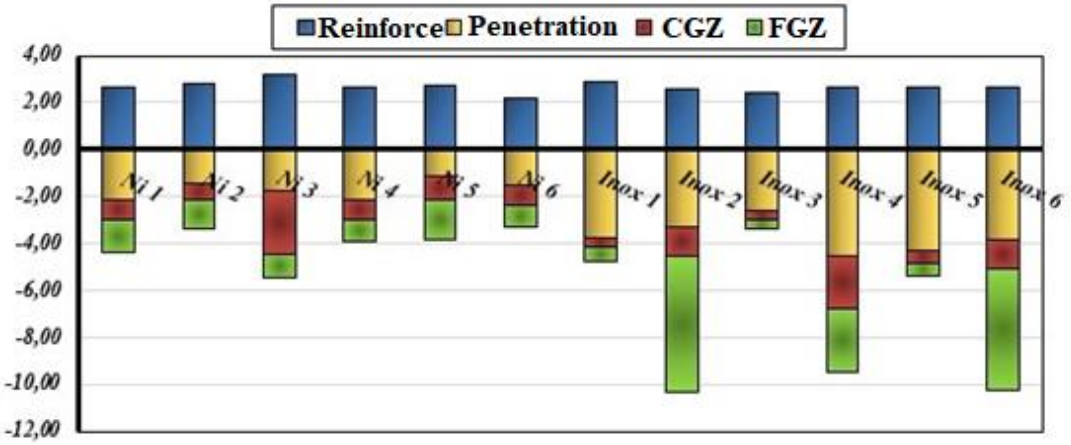

Figure 6: Higuchi modified diagram.

Once the Higuchi and Modified Higuchi diagrams were obtained, the decision diagrams were prepared to evaluate, by means of a graphic display, the approval of the parameters for the 2nd layer of coating according to the different criteria adopted by the Higuchi and Modified Higuchi tests. Figure 7 shows the decision diagram prepared considering the condition Ni 4 in the first coating layer.

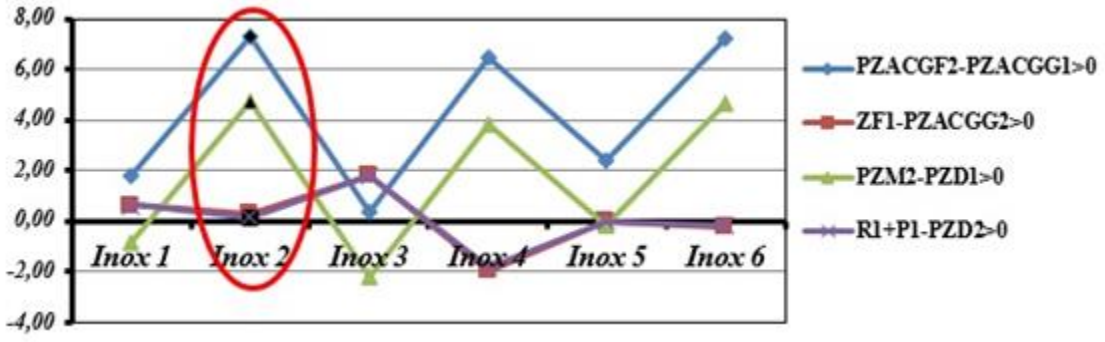

Figure 7: Decision diagram for condition Ni 4.

In the decision diagrams, conditions that lie below the reference line should not be used due to the risk of the extension of the hard zone of the 1st layer. Thus, analyzing the decision diagram in Figure 7, only Inox 2 condition proved satisfactory for overlapping the first layer with Ni 4 condition. Despite this, Inox 5 and 6 conditions were close to approval for the second layer.

3.2 Coating welding

Table 9 shows the two conditions selected by the decision diagrams for coating welding. Figure 8 illustrates the surface appearance and cross section of the coating.

Table 9: Coating welding conditions.

Coating	Condition	Temper-bead	Energy (J/mm)
Inox 2/Ni 4	Ni 4	1ª camada	710,10
	Inox 2	2ª camada	850,50

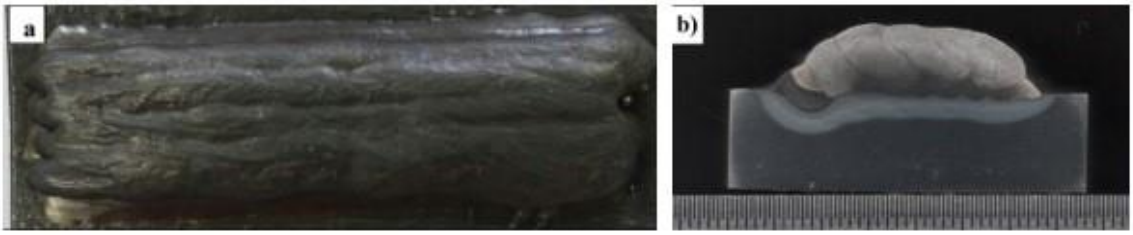

Figure 8: (a) Surface appearance and (b) macrography of the coating.

Analyzing the surface aspect and the macrography, no discontinuities capable of compromising the quality of the coating were observed. In order to evaluate the level of tempering acquired by the double layer technique, Figure 9 presents the microhardness profiles obtained for the Ni 4 isolated pass condition and for the Inox 2/Ni 4 coating.

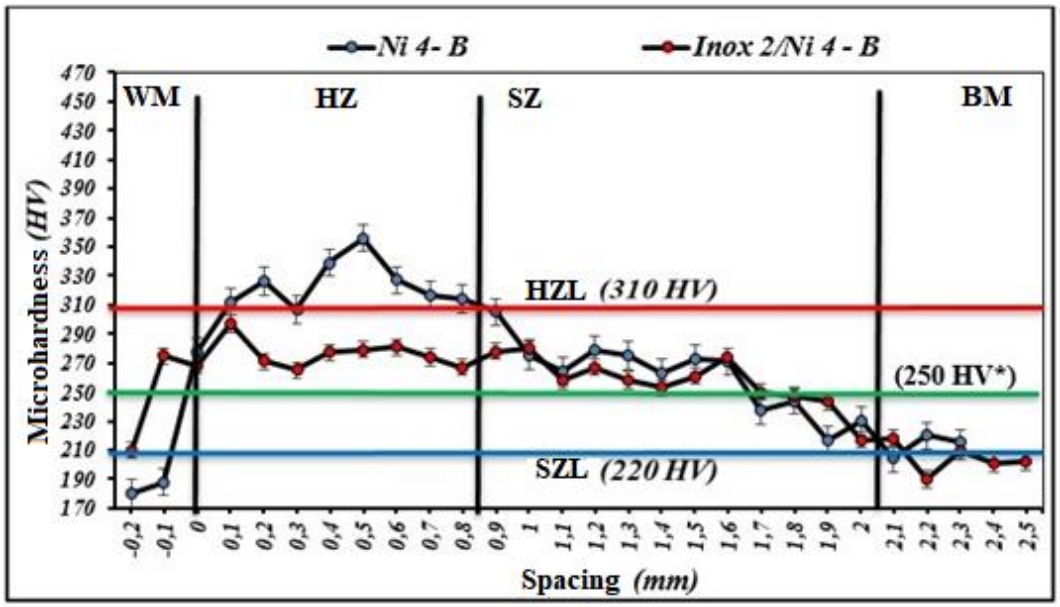

Figure 9: Microhardness profile for the isolated Ni 4 pass and the Inox 2/Ni 4 coating.

Figure 9 shows a considerable microhardness reduction for the Inox 2/ Ni 4 coating, indicating the effectiveness of the Higuchi and Modified Higuchi tests in selecting the conditions for the double layer technique. Despite the acquired tempering, the microhardnesses in the HAZ of the coating did not remain below the maximum microhardness level (250 HV) recommended by the NACE MR0175 standard (2005). Therefore, to meet the established requirements, one of the two coating samples was subjected to an SRHT. Figure 10 presents the microhardness profiles for the samples coated with (Inox 2/Ni 4 - HT) and without SRHT (Inox 2/Ni 4).

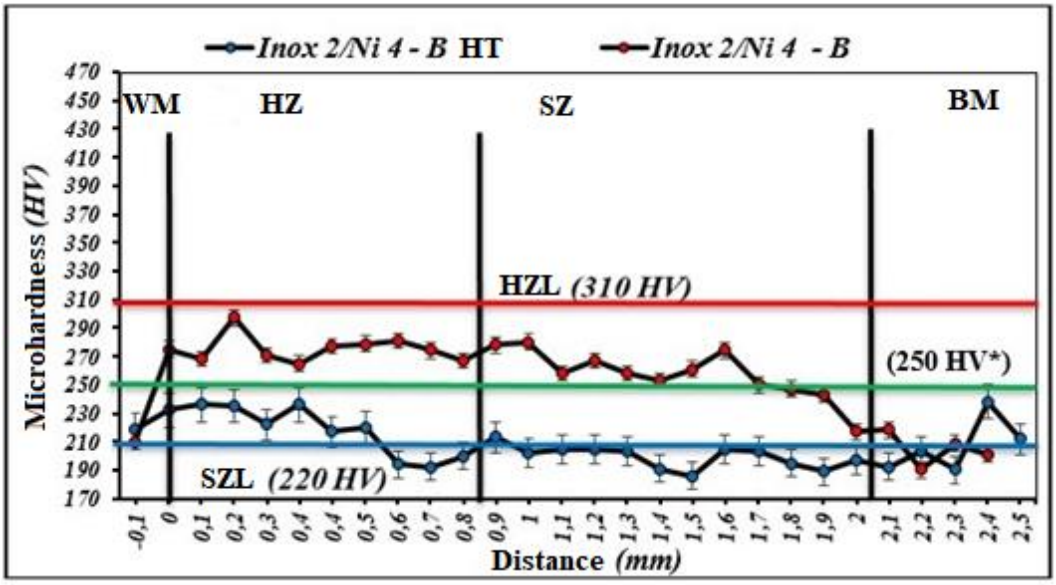

Figure 10: Microhardness profiles for the samples coated with (Inox 2/Ni 4 - HT) and without SRHT (Inox 2/Ni 4).

Analyzing the microhardness profiles in Figure 10, a significant reduction is observed for the heat-treated sample, including the levels recommended by NACE MR0175 (2005). Thus, it can be said that despite the proven effectiveness of the Higuchi and Modified Higuchi tests for the execution of the double layer technique, the level of tempering achieved is still insufficient to the point of completely eliminating the use of SRHT. However, the tempering observed with the technique by combining the nickel and stainless steel electrodes proved advantageous for two reasons. First, by combining the use of the two electrodes, instead of using only the nickel electrode, as usual, the cost of consumables falls dramatically since a nickel coil is worth up to three times more than a stainless steel coil. Second, even if the observed tempering does not reduce the microhardness to the maximum level recommended by NACE (2005), savings can be achieved, albeit small, in terms of manufacturing processes since the SRHT time and temperature can be lower because such significant tempering is no longer required.

4. CONCLUSION

Analyzing the microhardness results of the sample submitted to the double layer technique, the effectiveness of the Higuchi and Modified Higuchi tests is verified. However, clarified about a possible failure problem arising from improper structures and the influence of nickel alloys consumables to minimize the M zone formation show us that the maximum level of microhardness allowed by NACE MR0175 (2005) is not reached, the use of the double layer technique combined with the Higuchi and Modified Higuchi tests which were not completely eliminating the use of SRHT. However, the use of this methodology proved advantageous from an economic point of view by resulting in reduced costs with consumables and manufacturing processes.

5. ACKNOWLEDGEMENTS

We thank Prof. C. Mota for his contribution to the Welding Technology Research Group (GETSOLDA), PROEX-UFPa, CNPQ and the other students who helped with this article.

6. REFERENCES

AGUIAR, W.M. Soldagem do aço ABNT 4140 sem Tratamento Térmico posterior. Dissertação de Msc., UFC, Fortaleza, CE, Brasil, 2001.

DUPONT, J. N., KUSKO, C. S. Technical note: Martensite formation in austenitic/ferritic dissimilar alloy welds. Welding Journal. v. 86, n. 2, p. 51-54, 2007.

HIGUCHI, M.; SAKAMOTO, H.; TANIOKA, S. A study on weld repair through half bead method. IHI Engineering Review, v. 13(2), p. 14-19, 1980.

KEJELIN, N. Z., Buschinelli, A. J. A., and Pope, A. M. Influence of welding parameters on the formation of partially diluted zones of dissimilar metal welds. Soldagem e Inspeção 12(3): 195 - 203. 2007.

MIRANDA, H. C. Aplicação da dupla camada na soldagem de aços ASTM A516 Gr. 70. Tese de Doutorado, UFC,

Fortaleza, CE, Brasil, 2009.

NACE. Petroleum and natural gas industries – Materials for use in H2S – containing environments in oil and gas production Part 1: General principles for selection of cracking-resistant materials: NACE MRO175/ISO 15156-1:2001/Cor.:2005(E). U. S. A.: NACE. 2005.

OLIVEIRA, G. L. G., Soldagem dissimilar dos aços AISI 8630M e ASTM A182 F22 para aplicações subaquáticas, Tese de Doutorado, UFC, Fortaleza, CE, Brasil, 2013.

OMAR, A. A. Effects of welding parameters on hard zone formation at dissimilar welds. *Welding Journal*. v. 87, n.2, p 86s-93s, 1998.